Forensic Chemistry 14 (2019) 100160

Contents lists available at ScienceDirect

Forensic Chemistry

journal homepage: www.elsevier.com/locate/forc

The differentiation of 2,5-dimethoxy-N-(N-methoxybenzyl)phenethylamine (NBOMe) isomers using GC retention indices and multivariate analysis of ion abundances in electron ionization mass spectra

J. Tyler Davidson[a], Glen P. Jackson[a,b,*]

[a] Department of Forensic and Investigative Science, West Virginia University, Morgantown, WV 26506-6121, USA
[b] C. Eugene Bennett Department of Chemistry, West Virginia University, Morgantown, WV 26506-6121, USA

HIGHLIGHTS

- Identified the average retention indices for positional isomers of 25C- and 25I-NBOMe.
- Established the ortho effect as a mechanism to differentiate positional isomers.
- Demonstrated effectiveness of discriminant analysis for classification of NBOMes.
- When mass spectra are ideal classification rates exceed 99.9%.

ABSTRACT

Synthetic phenethylamine derivatives known as 2,5-dimethoxy-N-(N-methoxybenzyl)phenethylamines (NBOMes) are a common class of novel psychoactive substances (NPS) that are causing many accidental deaths across the United States. Many derivatives are now banned at the federal and state levels, but such control requires reliable identification of the different positional isomers. This manuscript helps establish retention indices and characteristic ion ratios that can be used to distinguish between the positional isomers of 25C-NBOMe and 25I-NBOMe. This manuscript also provides additional support for the ortho effect as a reliable, general, fragmentation mechanism to differentiate positional isomers of NBOMes in electron ionization (EI) mass spectra.

The retention indices and fragment ion abundances of the positional isomers of 25C-NBOMe and 25I-NBOMe were measured on two instruments using three different GC columns and parameters. The measured retention indices for the six compounds on three different 5% diphenyl columns are as follows: ortho-25C-NBOMe = 2614 ± 15; meta-25C-NBOMe = 2666 ± 13; para-25C-NBOMe = 2692 ± 13; ortho-25I-NBOMe = 2821 ± 16; meta-25I-NBOMe = 2877 ± 15; and para-25I-NBOMe = 2904 ± 12, where the errors represent the 95% confidence interval of the measurements. Principal component analysis (PCA) and canonical discriminant analysis (CDA) were used, respectively, to assess the variance and classification of NBOMe isomers based on the 15 most abundant ions relative to the base peak. The CDA classification accuracy for the six NBOMe compounds was 99.5% when the data set included spectra from three instrumental setups and the widest range of concentrations. Isomer classification was greater than 99.9% within an instrument and excluding low abundance spectra. These results support the use of chemometric approaches for the classification of unknown compounds, even when non-ideal lower-abundance spectra are used for classification.

1. Introduction

2,5-Dimethoxy-N-(N-methoxybenzyl)phenethylamines (NBOMes) are a class of synthetic phenethylamine derivatives, or novel psychoactive substances (NPSs), that have become increasingly popular in Europe, the United States, and Asia [1]. NBOMes are derivatives of the larger "2C" class of compounds, so named by Dr. Alexander Shulgin because of the two carbon atoms between the benzene ring and the amino group on the phenethylamine [1,2]. This 2C structure is common among other classes of drugs, such as amphetamines, catecholamines, cathinones, and many designer drugs since the 1970s. Over time there has been continued substitution to the generic phenethylamine structure, which has led to an abundance of 2C designer drugs. The substitutions made to the generic phenethylamine structure are responsible for the different physiological and psychological effects of 2C designer drugs [3].

NBOMes are low dosage hallucinogenic drugs, which has made them popular for recreational drug use [1]. Recognizing this trend, the Drug Enforcement Administration (DEA) temporarily placed three NBOMes in the Schedule I category of the Controlled Substances Act in November of 2013. The three NBOMes scheduled were 25I-, 25C-, and 25B-NBOMe, the three most common NBOMes on the market at the

* Corresponding author at: Department of Forensic and Investigative Science, West Virginia University, Morgantown, WV 26506-6121, USA.
E-mail address: glen.jackson@mail.wvu.edu (G.P. Jackson).

https://doi.org/10.1016/j.forc.2019.100160
Received 2 March 2019; Received in revised form 25 March 2019; Accepted 1 April 2019
Available online 01 April 2019

time [4]. This temporary scheduling was then extended in November of 2015 [5].

The first reported synthesis of an NBOMe was in 2003 by Dr. Ralf Heim of the University of Berlin who synthesized 25I-NBOMe as a pharmacological tool to study the 5-HT_{2A} receptor [1,2,4]. The 5-HT_{2A} receptor is also known to be responsible for the hallucinogenic effects of LSD [1]. However, LSD is only a partial agonist of the 5-HT_{2A} receptor, which means NBOMes actually produce a stronger hallucinogenic effect [6]. The hallucinogenic effects experienced from NBOMes are altered by the different substituents attached to their common structure [3,7].

NBOMes first became available over the internet in 2011 and were marketed as either legal highs or research chemicals that were not for human consumption [1]. Abusers of NBOMes are typically young males between the ages of 14–29 years old. When under the influence, abusers typically present symptoms of a serotonin-like syndrome, including violent physical and mental episodes that can be so extreme that they ultimately lead to death [1,2]. NBOMes are usually distributed as a powder or diluted to sub-milligram doses and laced into blotter paper [2]. The blotter paper is marked with identifying artwork and cut into tiny squares. These blotter paper squares are then administered sublingually, to gain direct entry into blood vessels under the tongue, or placed against the cheek to permit absorption through the cheek membranes in a method known as buccal administration. Another way to increase the bioavailability is to complex NBOMes with hydroxypropyl-beta-cyclodextrin (HPBCD) [1,8]. The price of a single 500 μg hit can be as low as $5 [1].

Between June of 2011 and June of 2013, 959 reports containing 25I, 25C, or 25B NBOMes from across 35 states were reported to the National Forensic Laboratory Information System (NFLIS) [4]. According to NFLIS, there were no submissions containing any type of NBOMe prior to June of 2011. Furthermore, the United States Customs and Border Protection data indicates bulk quantities of 25I, 25C, and 25B NBOMes have been seized from shipments originating from overseas, particularly from Asian countries [4]. Not only are NBOMes becoming increasingly available within the United States, but 11 states have implicated some combination of 25I, 25C, or 25B NBOMes in the death of at least 17 individuals. Despite an increasing effort to ban NBOMe use and trafficking in many countries, intoxications and fatalities have continued to increase worldwide [4]. Despite the decline in casework since being placed on the list of scheduled drugs, the DEA has reported more than 4000 cases involving 25I, 25C, or 25B NBOMes between January 2014 and April 2018 [9].

The increasing prevalence of NBOMe intoxications and fatalities has necessitated an increased emphasis on the characterization and identification of different NBOMes [10–14]. Several sub-classes of NBOMes have been characterized using liquid chromatography-tandem mass spectrometry (LC-MS/MS) and gas chromatography-electron ionization-mass spectrometry (GC-EI-MS) [15–21]. However, there is a general lack of information regarding the differentiation of positional isomers within a sub-class of each NBOMe.

This project describes the analysis and discrimination of ortho, meta, and para isomers of both 25C- and 25I-NBOMe to contribute to the understanding of NBOMe identifications, and it builds on the comprehensive study by Casale and Hays [2]. The development of characteristic retention indices for each isomer, as well as the variability of the relative ion abundances, is assessed by analyzing standards of each isomer on different instruments and on different days. The reason characterization of isomers is so important is because the substitution and arrangement of substituents dictates the hallucinogenic potency of these drugs [4]. The trends observed in this work could help provide more general rules for mass spectral interpretation of unknown NPSs in the future.

Principal component analysis (PCA) and canonical discriminant analysis (CDA) are used to visualize natural clustering of the data and to perform an assessment of the classification of NBOMe isomers based on the relative ion abundance data. PCA is an unsupervised data reduction technique that is commonly used to find natural patterns within a data set by maximizing the total variance between data points in the reduced dimensionality of multivariate data sets [22]. CDA is a supervised multivariate discriminant analysis technique that determines how best to separate or discriminate between two or more groups by maximizing the between-group variance and minimizing the within-group variance [23]. The application of multivariate analysis approaches to drug classification has been demonstrated by Setser and Waddell Smith [24], Harris et al. [25] and Bonetti [26].

In addition to conventional GC-EI-MS, this manuscript also compares fast GC–MS with traditional GC–MS. Fast GC–MS employs narrower and shorter columns, faster oven temperature ramp rates and higher carrier gas velocities to achieve faster separations, without sacrificing resolution [27]. The interest in fast GC–MS is primarily driven by the desire to reduce the cost per analysis through higher throughput, better utilization of high-cost instrumentation, and the need for fewer analysts [28]. Fast GC–MS has applications in the analysis of pesticides in fruit [29], contaminated drinking water [30], fatty acid methyl esters [31], antidepressants [32], and even field portable instrumentation [33]. Forensic applications of fast GC–MS include the screening of controlled substances in urine [34,35] and the analysis of seized drugs [36].

2. Methods

2.1. Background

This study employed two different GC–MS instruments, an Agilent Technologies 7890B GC/5977A MS and a PerkinElmer Clarus 680 GC/SQ8S MS. The Agilent instrument was operated under both traditional and fast GC conditions, whereas the PerkinElmer instrument was only operated under traditional GC conditions. The instrument conditions represented realistic conditions including split and splitless modes of sample introduction, conventional and narrow capillary columns, and different temperature gradients in oven temperature.

The concentrations of the samples analyzed were 12.5 ppm (0.0125 mg/mL), 125 ppm (0.125 mg/mL), and 1250 ppm (1.2 mg/mL) in HPLC grade methanol (Fisher Scientific). Each solution was analyzed at least twice a week for one or two months, depending on the technique and instrument availability. When the samples were not actively being analyzed, they were stored in a refrigerator to reduce sample degradation. A new cap was added after each injection to prevent solvent evaporation. For quality control, a chloroform blank, methanol blank, and an n-alkane ladder were analyzed at the beginning and end of each sequence. Between each sample analysis, a solvent rinse with both chloroform and methanol was used to clean the injection syringe. All samples were analyzed in a random order and a blank was run after each 1250 ppm solution to ensure that carryover did not occur. The randomization process was carried out using Microsoft Excel (Microsoft Corporation) version 14.

2.2. Chemicals and reagents

The ortho (o), meta (m), and para (p) isomers of 25C-NBOMe and 25I-NBOMe were provided by the DEA Special Testing and Research Laboratory [2]. Scheme 1 shows the generic NBOMe structure where the substituent at location R1, either chlorine or iodine, differentiates 25C-NBOMe and 25I-NBOMe, respectively, and the location of the methoxy substituent (R2, R3, or R4) determines the positional isomer. The methanol and chloroform solvents used for blanks were supplied by Fisher Scientific (Palo Alto, CA). The C7-C30 n-alkane ladder was supplied by Supelco (Bellefonte, PA).

2.3. Agilent fast GC–MS method

Fast GC on the Agilent system used a VF-5MS column of dimensions

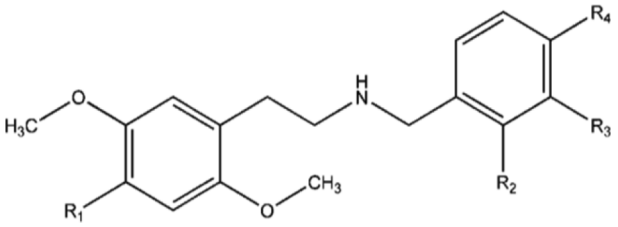

Scheme 1. Chemical structure of a generic NBOMe [2].

10 m × 0.15 mm × 0.15 µm. The GC–MS parameters were as follows: an injection volume of 1 µL, an injection temperature of 250 °C and a 100:1 split ratio. The initial oven temperature was 150 °C, which was ramped to 280 °C at 25 °C/min, then held for 1 min. The carrier gas was ultra-high-purity helium (Matheson) with a flow rate of 1 mL/min. The mass spectrometer was scanned from *m/z* 25–500 after a 0.5 min solvent delay. The transfer line and ion source temperatures were 280 °C and 250 °C, respectively. The scan rate was 1500 Da/sec and the total run time for the fast GC–MS analysis was 6.20 min.

2.4. Agilent traditional GC–MS method

Traditional GC on the same Agilent system used an HP-5 30 m × 0.25 mm × 0.25 µm column for separation. The GC–MS parameters were as follows: an injection volume of 1 µL, an injection temperature of 250 °C and a 40:1 split ratio. The initial oven temperature was 150 °C, which was ramped to 280 °C at 15 °C/min, then held for 3 min. The carrier gas was ultra-high-purity helium (Matheson) with a flow rate of 1 mL/min. The mass spectrometer was scanned from *m/z* 25–500 after a 2 min solvent delay. The transfer line and source temperatures were 280 °C and 250 °C, respectively. The scan rate was 1500 Da/sec and the total run time for the Agilent traditional analysis was 12.67 min.

2.5. PerkinElmer traditional GC–MS method

The column used for the PerkinElmer traditional analysis was a ZB-5MS column of dimensions 20 m × 0.18 mm × 0.18 µm. The GC–MS parameters were as follows: an injection volume of 1 µL, an injection temperature of 250 °C and analyzed in splitless mode. The initial oven temperature was 150 °C, which was ramped to 280 °C at 15 °C/min, then held for 3 min. The carrier gas was ultra-high-purity helium (Matheson) with a flow rate of 1 mL/min. The mass spectrometer was scanned from *m/z* 25–500 after a 2 min solvent delay. The transfer line and source temperatures were 250 °C and 200 °C, respectively. The scan rate was 1800 Da/sec and the total run time for the PerkinElmer traditional analysis was 12.67 min.

2.6. Data analysis

The retention times were extracted via auto-integration at the peak apex. MSD ChemStation version C.01.01 or TurboMass version 6.1.0 were used to export the retention time information as well as the extracted ion abundances into Microsoft Excel (Microsoft Corporation) version 14. Excel and SPSS version 25 were used for the remaining data analysis, including the normalization of the 15 most abundant ions to the *m/z* 121 base peak. The most abundant fragments were used to minimize random variance; it is well-known that the least abundant ions in a spectrum display larger range measurement uncertainty than the most abundant ions in a spectrum [37,38]. Also, anecdotal evidence suggests that EI mass spectra will almost always contain at least 15 ions in a spectrum, and McLafferty et al. have demonstrated that using 15 ions in a spectral search algorithm can be at least 87% as accurate as using all the ions in a spectrum [39]. The relative ion abundances were used as covariates in principal component analysis (PCA) and canonical discriminant analysis (CDA), respectively, to examine any natural clustering and the classification accuracy of the isomers based on the relative ion abundances.

The inclusion of an n-alkane ladder enabled the calculation of retention indices (RI) for each isomer using each method [40]. The equation used to calculate the retention indices is shown below in Eq. (1), and the equation uses the retention time of the unknown ($t_{r(x)}$), the retention time of the adjacent n-alkane with a shorter retention time ($t_{r(n)}$), the adjacent n-alkane with a longer retention time ($t_{r(n+1)}$), and the number of carbon atoms in the adjacent n-alkane with a longer retention time (n). For the purpose of providing retention indices independent of instrumental setup the 95% confidence interval retention index for each isomer was calculated with the combined data.

$$RI = 100n + 100\left(\frac{t_{r(x)} - t_{r(n)}}{t_{r(n+1)} - t_{r(n)}}\right) \quad (1)$$

3. Results and discussion

3.1. Chromatographic results

Fig. 1 shows total ion chromatogram (TIC) of the separation of all six isomers performed with both Agilent fast GC–MS and Agilent

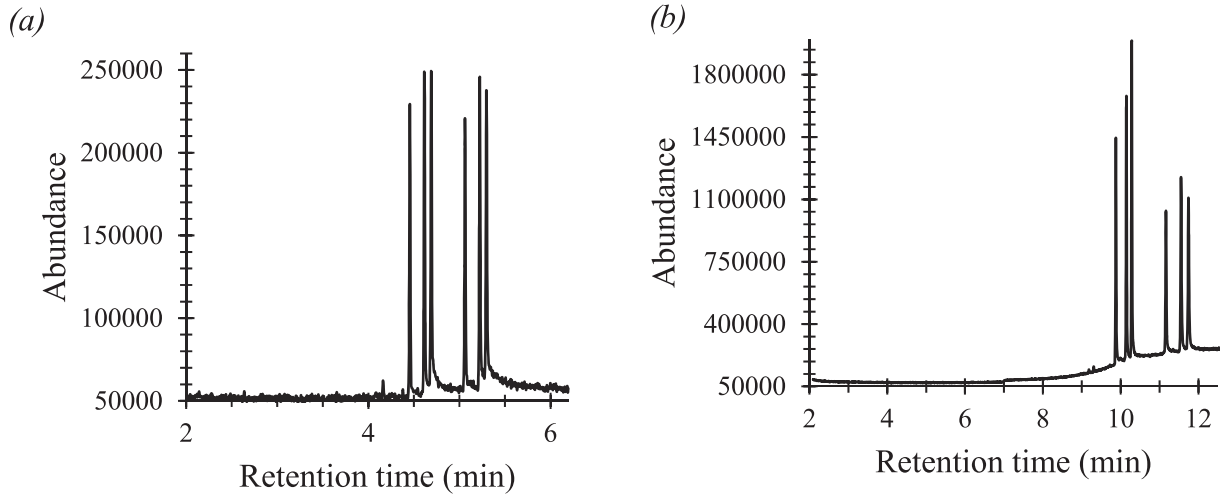

Fig. 1. Comparison of the total ion chromatograms of a 125 ppm mixture of all six compounds using (a) Agilent fast GC–MS and (b) Agilent traditional GC–MS. The elution order is the same in both chromatograms: o-25C-NBOMe, m-25C-NBOMe, p-25C-NBOMe, o-25I-NBOMe, m-25I-NBOMe, p-25I-NBOMe.

traditional GC–MS. Each isomer is present at 125 ppm in the mixture. The separation was performed in 6.20 min for the fast analysis and 12.67 min for the traditional analysis. Several minor peaks were observed that are consistent with degradation products or column/septum bleed. Two main trends are notable in these exemplar chromatograms. First, the elution of each NBOMe is always in the order of ortho, meta, para, and second, the 25C-NBOMe isomers have a shorter retention time than the 25I-NBOMe isomers.

An important aspect in the argument for the implementation of fast GC–MS in crime labs is the demonstration of the decrease in analysis time without the loss of chromatographic separation efficiency. Whereas the definition of baseline resolution (R = 1.50) was only routinely met for the ortho- and meta- isomers of each NBOMe in each mode of GC analysis, Fig. 1 shows that the resolution is visually sufficient to permit differentiation between the six compounds. The qualitative identification of these six NBOMes can be accomplished more than twice as fast with fast GC compared to traditional GC; i.e. > 50% shorter retention times. The full width at half maximum (FWHM) for the traditional GC peaks are on average 1.62 times larger than the fast GC peaks, whereas the peak width at the base is on average 5.60 times larger for the traditional GC than fast GC peaks. These non-systematic reductions in retention times and peak widths reveal that fast GC peaks are more symmetrical that the traditional GC peaks. Whether one uses the FWHM or peak width at the base for efficiency calculations [41], the traditional GC provides around 1.4 times more theoretical plates than fast GC, so is more efficient. However, the retention time variance here is on the order of 0.05%, which is typical of a crime laboratory [38], and adequate for discrimination of these six NBOMe compounds.

The measured retention times can be standardized/normalized to the retention times of n-alkanes to generate a retention index, as described in Eq. (1). The derived retention index is designed to permit direct comparisons of retention behavior between different instruments. However, deviations in retention index measurements on the order of 0.35% are common [42]. Retention index measurements are particularly helpful in casework situations in which the EI mass spectrum may provide more than one possible identity from a database search, but only one possible identity when the retention index is taken into account. In this manner, retention indices add an additional level of confidence against false positive identifications. To take advantage of these combined benefits, NIST employs a combination of retention index similarity and mass spectral similarity to great effect in their AMDIS compound identification software [43].

Fig. 2 shows the results for the combined retention indices across all methodologies studied. The boxes show the interquartile range of the data and the whiskers show the upper and lower levels for the non-rejected data points. Three data points were rejected based on obvious grouping with other isomers indicative of a clerical error. Even with the increased uncertainty caused by the use of different instrument setups, the difference between isomers is clear. An even better separation of retention indices is observed when the retention indices are calculated within a single instrument (Fig. S1). The 95% confidence intervals for the retention indices of the combined data are as follows: o-25C-NBOMe = 2614 ± 15; m-25C-NBOMe = 2666 ± 13; p-25C-NBOMe = 2692 ± 13; o-25I-NBOMe = 2821 ± 16; m-25I-NBOMe = 2877 ± 15; and p-25I-NBOMe = 2904 ± 12, with all values significantly different at the 95% confident level based on pairwise t-tests.

3.2. Mass spectrometry results

Fig. 3 shows the results for the three 25C-NBOMe isomers analyzed with the Agilent instrument operated in fast GC mode at 1250 ppm. Spectra for the 25I isomers are shown in Fig. S2. For each isomer in Fig. 3, the base peak is *m/z* 121 and the molecular ions are below the detection threshold. The ions at *m/z* 150 and *m/z* 91 are the second and third most abundant ions, respectively. The spectra are truncated to the window *m/z* 50 to *m/z* 300 to eliminate most of the background ions. One contamination peak that is still present is at *m/z* 207, which is known to originate from column and septum bleed. The relative abundance of the *m/z* 150 and *m/z* 91 peaks are of particular importance because these two ions can help distinguish the positional isomers of 25C-NBOMe [2].

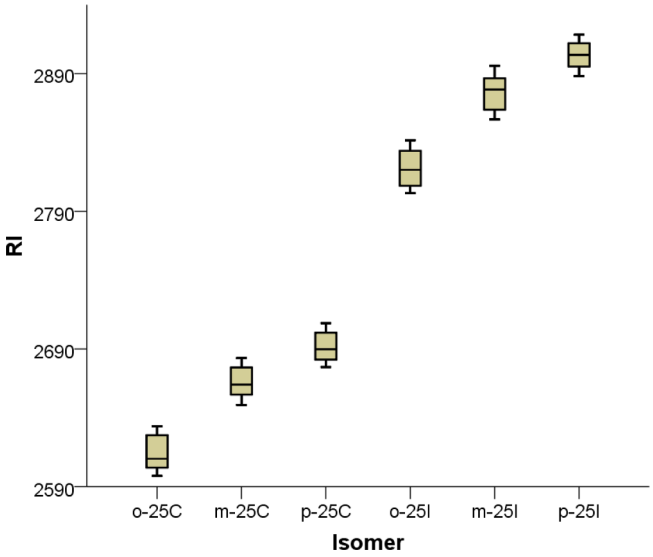

Fig. 2. Box and whisker plot showing the combined (across three concentrations) retention indices results for all methodologies studied.

There are several trends of note in the example spectra of Fig. 3 (and Fig. S2). First, none of the 25C-NBOMe or 25I-NBOMe isomers produced a molecular ion peak. These findings are consistent with the works of Zuba and Sekula [44] and Casale and Hays [2], although the molecular ions are occasionally detectable in the range of 0.05–1.0% relative abundance in the previous studies.

Another trend in the current work is that the fragment at *m/z* 91 is always most abundant for the ortho isomer and least abundant for the para isomer of both 25C-NBOMe and 25I-NBOMe. This phenomenon, related to the ortho effect, has been described previously by Harris et al. for the synthetic cannabinoid JWH 250 [25] and observed experimentally for NBOMe isomers by Casale and Hays [2]. Additionally, there are significant differences in the relative abundance of *m/z* 150 and *m/z* 91, and unique ions are also present in the spectra that could be used to indicate the presence of 25C-NBOMe vs 25I-NBOMe. As described in detail below, the most discriminating ions are *m/z* 185 & 186 for the 25C-NBOMe spectra and *m/z* 277 & 278 for the 25I-NBOMe spectra.

3.3. Multivariate analysis

PCA was used to analyze the natural clustering of the relative ion abundances based on the isomer factor. A correlation plot between the *m/z* variables and the first two PCs shows which ions contributed significantly to the natural clustering. Fig. S3 shows the PCA and correlation plots. Based on the strong natural clustering that is observed between the relative ion abundances and the isomer factor, CDA was used to analyze the classification of the NBOMes into six isomer groupings based on the relative ion abundances.

Fig. 4a shows a CDA plot of the first two discriminant functions when the 15 most abundant ions are used as variables to discriminate between the six different isomer groupings. Fig. 4b shows the ion correlation values with the same discriminant functions. The group centroids for each isomer grouping are shown as black squares. The correlation plot in Fig. 4b provides insight into which ions correlate with each isomer grouping. For example, *m/z* 278 (bottom center orange

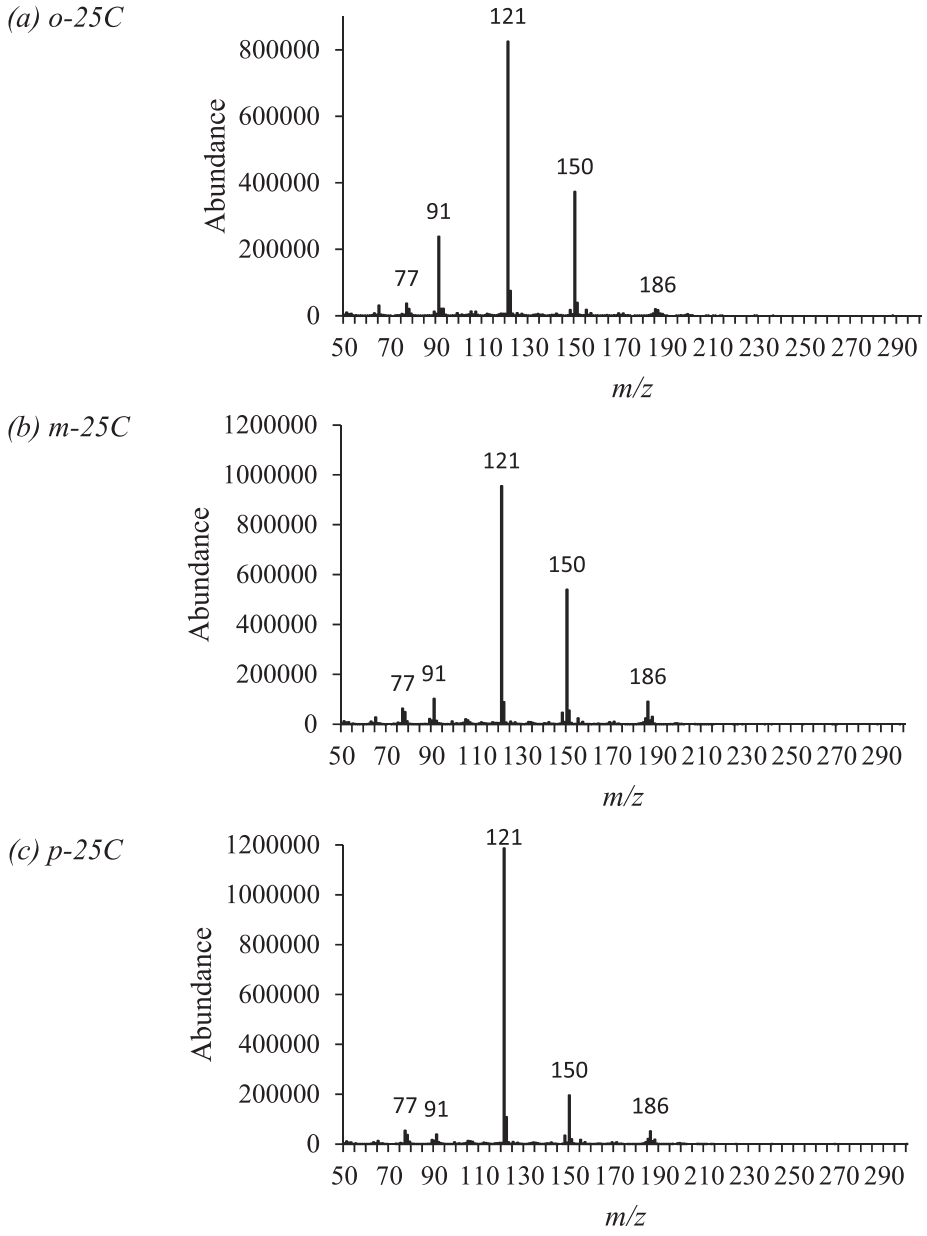

Fig. 3. 1250 ppm 25C-NBOMe Agilent fast GC–MS spectra corresponding to (a) o-25C, (b) m-25C, and (c) p-25C.

circle) has the strongest negative correlation with the second discriminant function. This fragment correlates with the 25I-NBOMe positional isomers. Likewise, the fragment at *m/z* 186 (top left gray circle) has the strongest positive correlation with the second discriminant function, which correlates with the 25C-NBOMe positional isomers. The fragments at *m/z* 150 and *m/z* 91 have the strongest positive correlation with the first discriminant function, which correlates strongest with the ortho isomers of 25C-NBOMe and 25I-NBOMe.

SPSS software was used to generate classification results based on the predicted group membership for both the original and the cross-validated grouped cases. The original grouped cases refer to the situation where the same observations are used for both the training set and validation set. Leave-one-out cross-validation (LOOCV) refers to the situation wherein each observation is used sequentially for external validation. The remaining spectra are used as the training set. This process is then repeated so that each spectrum serves as an external validator once.

When all three sample concentrations were included, 99.5% of the cases were correctly classified for both the original and cross-validated groupings. Of the seven cases where misclassification occurred, only a single misclassification was between positional isomers within a specific compound; i.e. six of the seven misclassifications could be distinguished with RI. However, based on the spread of the natural clustering seen in the PCA plot and the variation observed in the CDA plot, the data showed that the lowest concentration samples often contained peak drop-out and larger-than-average deviations from the typical peak abundances. The irreproducibility of low-abundance spectra has been reported before [26,37], and for this reason the lowest concentration samples were removed from the data set to generate a 'premium' data set, which consisted of only the 125 ppm and 1250 ppm samples.

Fig. S4 contains the PCA and ion correlation plots generated for the premium data set. The premium data set in Fig. S4 shows the same natural clustering of each isomer grouping, but slightly better separation between the isomer groupings than when the low-abundance spectra were included in data set (i.e. Fig. S3).

Fig. 5a shows the a CDA plot of the first two discriminant functions when the 15 most abundant ions are used as variables to discriminate between the six different isomer groupings of the premium data set.

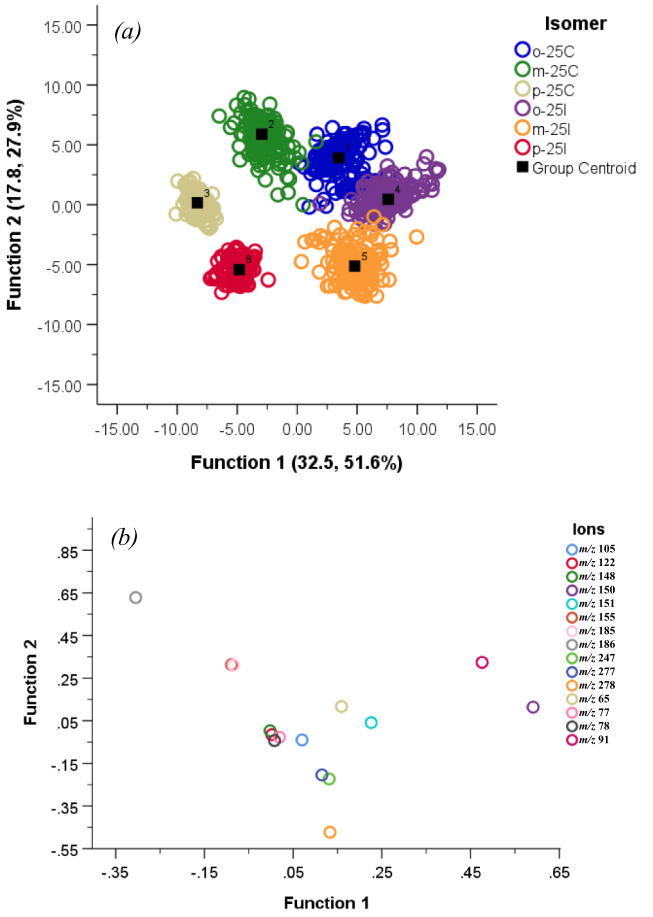

Fig. 4. Canonical discriminant analysis (CDA) showing the classification of (a) the NBOMe isomer groupings based on the relative ion abundances, and (b) the structure matrix correlation values where function 1 and 2 are the pooled within group correlations between the discriminant variables and the standardized canonical discriminant functions. N = 1514 for the entire data set, which includes concentrations of 12.5 ppm, 125 ppm and 1250 ppm.

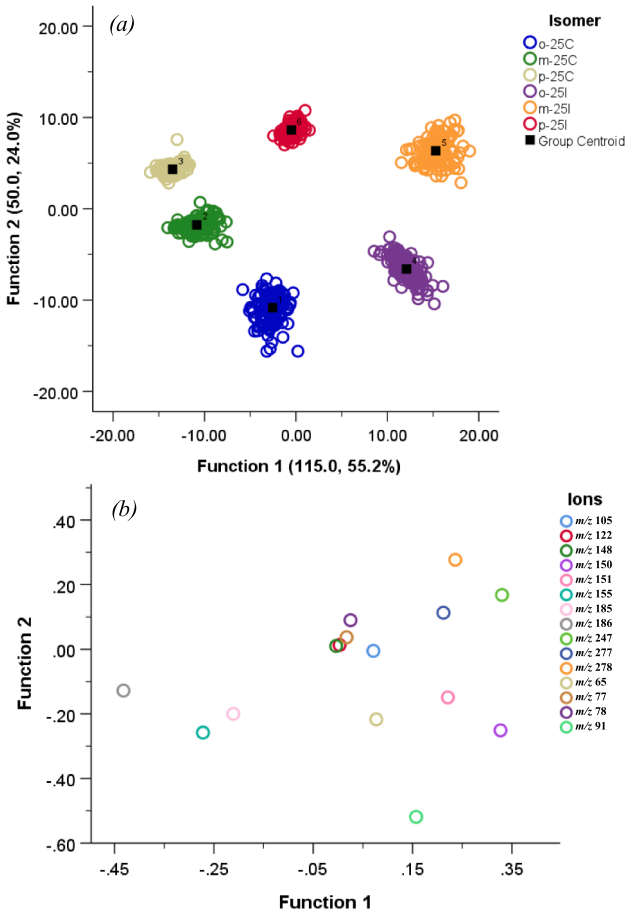

Fig. 5. Canonical discriminant analysis (CDA) showing (a) the classification of the NBOMe isomer groupings based on the relative ion abundances of 15 ions, and (b) the structure matrix correlation values where function 1 and 2 are the pooled within group correlations between the discriminant variables (*m/z* abundances) and the standardized canonical discriminant functions. N = 1026 for the premium data set, which contains only the 125 ppm and 1250 ppm samples.

This data set excludes the 12.5 ppm data. Fig. 5b shows the ion correlation values with the same discriminant functions. The group centroids for each isomer grouping are shown as black squares. In contrast to the CDA plot using all three concentrations (Fig. 4a), the premium data set shows better separation between the isomer grouping factors. The correlations in Fig. 5b again show that the 25C-NBOMe and 25I-NBOMe positional isomers are correlated with the fragments at *m/z* 186 and *m/z* 278, respectively, and the ortho isomers correlate with *m/z* 91 and *m/z* 150.

The classification results based on the predicted group membership for both the original and the cross-validated grouped cases were generated using SPSS software. The classification results for the premium data set demonstrated that 100.0% of the original grouped cases were classified correctly and 99.9% of the cross-validated grouped cases were classified correctly. The lone misclassification was between an ortho and meta isomer of 25I-NBOMe. The premium data set provides superior classification results compared to the full data set, and this result indicates that when the two highest concentration samples are used for spectral comparisons, classification rates are nearly errorless for these six compounds. Similarly, when CDA classification is used for determining group membership from the data collected within only a single instrument, the classification results are 100.0% for both the original grouped and cross-validated grouped cases (Fig. S5). Fig. S6 (25C-NBOMe) and Fig. S7 (25I-NBOMe) demonstrate the CDA classification results for the three positional isomers when classified within a single compound. The separation between groups is enhanced and the resulting classification is 100.0% for both the original and cross-validated groups. Given the ease of distinguishing between 25C and 25I isomers, these superior CDA models and prediction rates (100.0%) offer a more realistic comparison to casework situations.

Based on the structure matrix correlation values from the CDA classification *m/z* 91, *m/z* 150, *m/z* 186, and *m/z* 278 are major contributors towards the classification of NBOMes. The relationship between the intensity of these four ions and the *m/z* 121 base peak allows for the differentiation of the positional isomers of 25C-NBOMe and 25I-NBOMe. The relative abundance of *m/z* 91 and *m/z* 150 helps with the differentiation of the ortho, meta, and para isomers of these two NBOMe compounds. For example, Fig. 6a and b show the box and whisker plots for the relative ion abundances of fragment ions at *m/z* 91 and *m/z* 150 for the positional isomers of both 25C-NBOMe and 25I-NBOMe. The ortho effect is highlighted in Fig. 6a wherein the relative abundance of the *m/z* 91 fragment ion is always most abundant for the ortho isomer and least abundant for the para isomer. Fig. 6b also shows visual differences in the relative ion abundance of the fragment at *m/z* 150 for these two compounds. Fig. 6a and b include the variance caused by a factor of 10 range in concentration and differences caused by different instruments and settings. Even with these additional sources of variance, the positional isomers display visual differences in the relative abundance of the *m/z* 91 and *m/z* 150 fragment ions. In a crime laboratory, the performance of the mass spectrometer and the

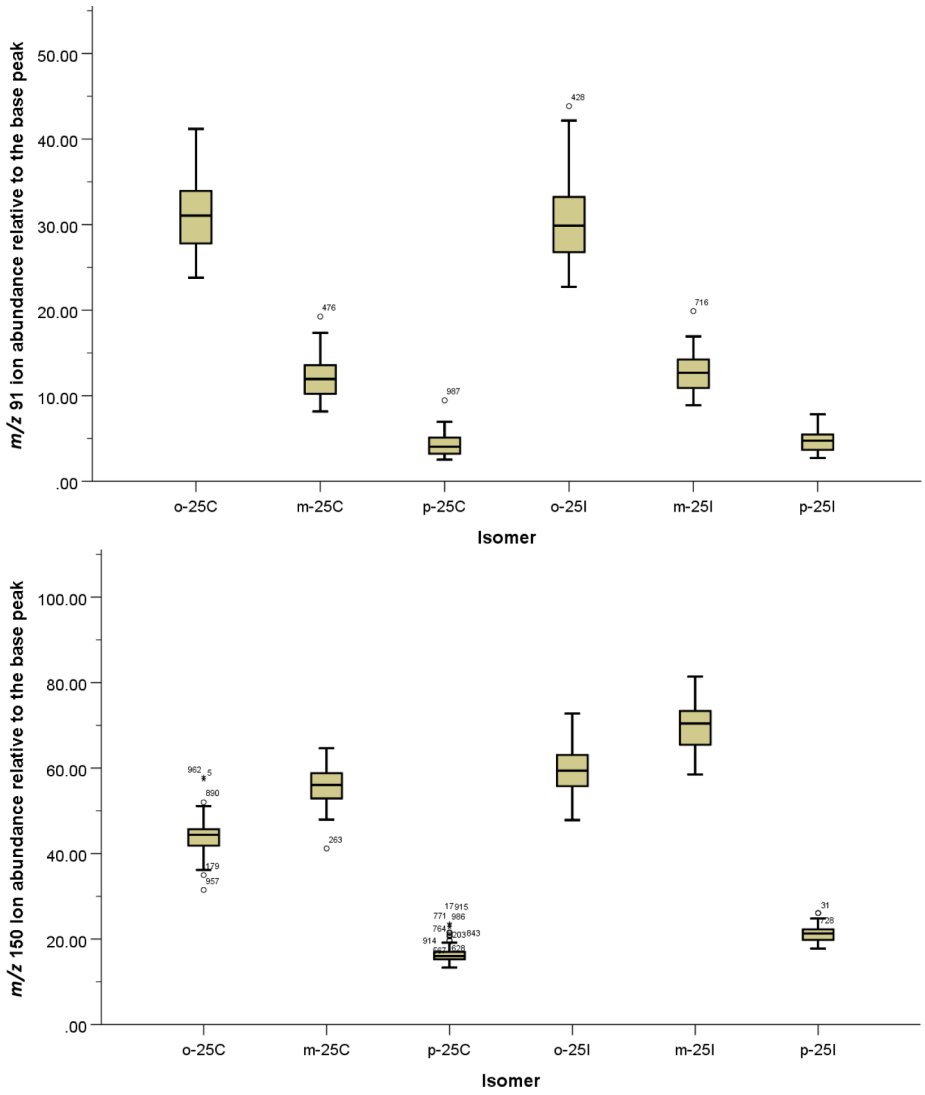

Fig. 6. Box and whisker plot showing the relative ion abundance for the fragments at (a) *m/z* 91 (b) *m/z* 150 for the ortho, meta, and para isomers of 25C-NBOMe and 25I-NBOMe.

concentration of the unknown sample are likely to contain more variance than in a typical research setting, so, from a practical perspective, it is important to establish—as we have done here—that isomer differentiation is still possible even when the known sources of variance are not tightly controlled.

To contribute to the knowledge about the positional isomers of 25C-NBOMe and 25I-NBOMe 95% confidence intervals were calculated for the relative ion abundances of the *m/z* 91, *m/z* 150, *m/z* 186, and *m/z* 278 characteristic ions ratios. These four discriminating ions were selected from the 15 most abundant ions for each isomer based on the structure matrix correlation values from the CDA classification. Significant differences between group means were detected for all pairwise comparisons using t-tests, except for the ortho isomers of 25C-NBOMe and 25I-NBOMe and the ortho, meta, and para isomers of 25C-NBOMe and 25I-NBOMe for *m/z* 186 and *m/z* 278, respectively. Table S1 shows the calculated 95% confidence interval of the mean abundances for these four characteristic ions. The mean abundance of all six isomers can be differentiated based on these statistically significant 95% confidence interval relative ion abundances. However, it is important to emphasize that these 95% confidence interval characteristic ion ratios of the mean are not to be used as acceptance criteria for the identification of 25C-NBOMe or 25I-NBOMe positional isomers, but rather an assessment of the population mean for each characteristic ion identified over the course of more than 250 replicate samples.

For the purpose of compound differentiation, the ion abundances at *m/z* 186 and *m/z* 278 are the most discriminating because they are related to the 25C-NBOMe and 25I-NBOMe isomers, respectively. The correlation plot for the premium CDA data in Fig. 5b shows that *m/z* 278 correlates most strongly with the 25I isomers in the upper right-hand quadrant of the CDA plot, and *m/z* 186 correlates most strongly with the 25C isomers on the left-hand side of discriminant function 1. The two ions with the most significant impact on the differentiation of the NBOMe positional isomers analyzed are *m/z* 91 and *m/z* 150. These two ions are the second and third most abundant fragments for the six NBOMes analyzed, after the base peak at *m/z* 121, and they have strong correlations to discriminant functions 1 and 2 in the entire NBOMe data set and the premium NBOMe data set.

3.4. Structural characterization

The next step is to understand why the relative ion abundance of these four ions are characteristic for the six NBOMe compounds. Fig. 7 shows the proposed mechanisms for the generation of these four characteristic ions, where each pathway is highlighted in a different color and the "X" represents either chlorine—for 25-C isomers—or iodine for the 25-I isomers. The presence of *m/z* 186 indicates the 25C-

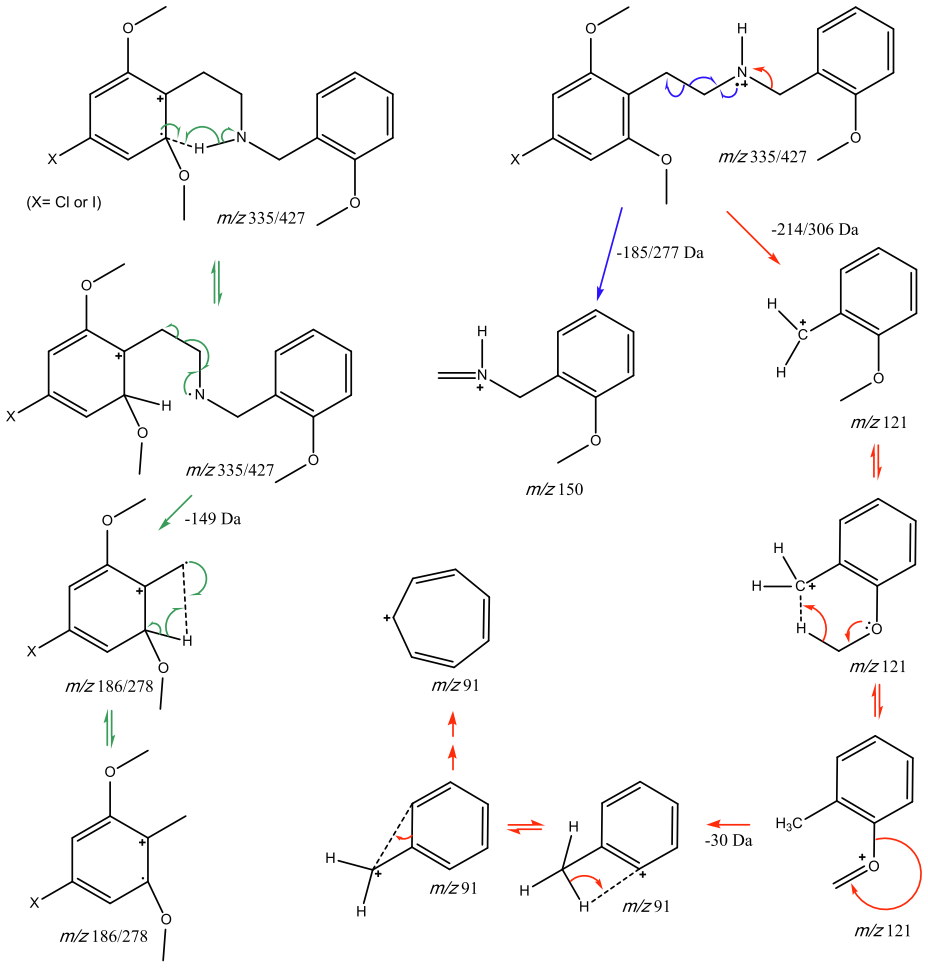

Fig. 7. Proposed mechanism for the generation of the *m/z* 91, *m/z* 150, *m/z* 186, and *m/z* 278 characteristic ions from ortho isomers of NBOMe.

NBOMe isomers and *m/z* 278 indicates the 25I-NBOMe isomers. A common mechanism forms both ions. This mechanism, highlighted in green, involves a McLafferty rearrangement and is not very favorable; the relative ion abundances of these fragments are typically less than 15%. However, the positional isomers can be distinguished based on the favorability of other pathways, such as through the formation of a tropylium ion at *m/z* 91 from substituted aromatic methyl ethers [45–47].

The red arrows show the most favorable pathway for all six NBOMes, which is through the fragment at *m/z* 150 with a simple radical-directed α-cleavage adjacent to the ionized nitrogen atom. The combination of the relative ion abundance of *m/z* 150 and *m/z* 91 allows the positional isomers of both 25C and 25I-NBOMe to be easily distinguished. The base peak at *m/z* 121 forms through charge-directed σ-bond cleavage adjacent to the nitrogen radical, and the relative abundance of the tropylium ion (*m/z* 91) is based on the proximity of the methoxy substituent to the carbocation. The rearrangements necessary to eliminate the 30 Da formaldehyde neutral from the methyl ether is strongly favored when the methoxy group is adjacent (ortho) to the substituent group [25,48–52]. The mechanistic understanding of the origin of these characteristic ions provides the chemical knowledge in support of the multivariate classification and structure matrix correlation conclusions.

4. Conclusions

The determination of distinct retention indices and characteristic ion ratios is an important contribution to the knowledge about NBOMes. The ability to differentiate between NBOMe isomers with retention indices allows crime labs using different instrumental setups and parameters to differentiate between the positional NBOMe isomers. The demonstration of fast GC nearly doubling the speed of analysis without a significant loss of chromatographic separation efficiency provides further support for the application of fast GC–MS to crime laboratories.

The identification of four characteristic ion ratios that allow for the differentiation of population mean abundances for the six NBOMes analyzed is also a significant contribution to the knowledge about NBOMes. However, these 95% confidence interval characteristic ion ratios of the mean are not to be applied as acceptance criteria within a crime lab, but rather an assessment of the population mean for each characteristic ion identified over the course of more than 250 replicates. This manuscript also further establishes the ortho effect as a reliable fragmentation mechanism to differentiate positional isomers of NBOMes in electron ionization (EI) mass spectra.

The inclusion of the classification study performed with the CDA relative ion abundance results indicates that at higher concentrations, where less variability is present, the classification of the positional isomers of 25C-NBOMe and 25I-NBOMe increased to nearly errorless classification. Classification rates were also errorless when data from within a single instrument was used for the CDA classification. However, even when poor quality, low concentration samples were included in the training and validation test sets, the classification rate was still better than 99.5% accurate. These results demonstrate that the use of multivariate classification shows great promise for the differentiation and possible identification of similar chemical structures based on the EI-MS mass spectral fragmentation.

Acknowledgements

This project was supported by grant number 2018-75-CX-0033, awarded by the National Institute of Justice, Office of Justice Programs, and U.S. Department of Justice. The opinions, findings, and conclusions or recommendations expressed in this publication are those of the authors and do not necessarily reflect the views of the Department of Justice.

Appendix A. Supplementary data

Supplementary data to this article can be found online at https://doi.org/10.1016/j.forc.2019.100160.

References

[1] J.L. Poklis, S.A. Raso, K.N. Alford, A. Poklis, M.R. Peace, Analysis of 25I-NBOMe, 25B-NBOMe, 25C-NBOMe and other dimethoxyphenyl-N-[(2-Methoxyphenyl) methyl]ethanamine derivatives on blotter paper, J. Anal. Toxicol. 39 (8) (2015) 617–623.
[2] J.F. Casale, P.A. Hays, Characterization of eleven 2,5-dimethoxy-N-(2-methoxybenzyl)phenethylamine (NBOMe) derivatives and differentiation from their 3- and 4-methoxybenzyl analogues – Part I, Microgram 9 (2) (2012) 84–109.
[3] S.J. Stellpflug, S.E. Kealey, C.B. Hegarty, G.C. Janis, 2-(4-Iodo-2,5-dimethoxyphenyl)-N-[(2-methoxyphenyl)methyl]ethanamine (25I-NBOMe): clinical case with unique confirmatory testing, J. Med. Toxicol. 10 (1) (2014) 45–50.
[4] Schedules of Controlled Substances: Placement of Three Synthetic Phenethylamines Into Schedule I, Fed. Reg., Drug Enforcement Administration, 2013.
[5] Schedules of Controlled Substances: Extension of Temporary Placement of Three Synthetic Phenethylamines in Schedule I. Final order., Fed. Regist., Drug Enforcement Administration, 2015.
[6] G.J. Marek, G.K. Aghajanian, LSD and the phenethylamine hallucinogen DOI are potent partial agonists at 5-HT2A receptors on interneurons in rat piriform cortex, J. Pharmacol. Exp. Ther. 278 (3) (1996) 1373–1382.
[7] D. Sánchez Robayo, A.W. Garzón Mendez, F.G. Taborda Ocampo, M. Rosero Moreano, Analysis of blotter papers employed in the commercialization of new hallucinogenic substances of the 2,5-dimethoxy-n-(2-methoxybenzyl) phenethylamine series seized in the City of Bogotá by applying gas chromatography coupled to a selective mass ion trap detector, J. Braz. Chem. Soc. (2016).
[8] C.A. Stuenkel, R.E. Dudley, S.S. Yen, Sublingual administration of testosterone-hydroxypropyl-beta-cyclodextrin inclusion complex simulates episodic androgen release in hypogonadal men, JCEM 72 (5) (1991) 1054–1059.
[9] Drug Enforcement Administration Diversion Control Division Drug & Chemical Evaluation Section: 25I-NBOMe, 25C-NBOMe, and 25B-NBOMe, 2018.
[10] A. Anstett, F. Chu, D.E. Alonso, R.W. Smith, Characterization of 2C-phenethylamines using high-resolution mass spectrometry and Kendrick mass defect filters, Forens. Chem. 7 (2018) 47–55.
[11] É.N. Oiye, M.T.J. Katayama, M.F.M. Ribeiro, M.F. de Oliveira, Electrochemical analysis of 25H-NBOMe by square wave voltammetry, Forens. Chem. 5 (2017) 86–90.
[12] I. Papoutsis, P. Nikolaou, M. Stefanidou, C. Spiliopoulou, S. Athanaselis, 25B-NBOMe and its precursor 2C-B: modern trends and hidden dangers, Forensic Toxicol. 33 (1) (2014) 1–11.
[13] S. Botch-Jones, J. Foss, D. Barajas, F. Kero, C. Young, J. Weisenseel, The detection of NBOMe designer drugs on blotter paper by high resolution time-of-flight mass spectrometry (TOFMS) with and without chromatography, Forensic. Sci. Int. 267 (2016) 89–95.
[14] D. Zuba, K. Sekula, A. Buczek, 25C-NBOMe–new potent hallucinogenic substance identified on the drug market, Forensic Sci. Int. 227 (1–3) (2013) 7–14.
[15] R.D. Johnson, S.R. Botch-Jones, T. Flowers, C.A. Lewis, An evaluation of 25B-, 25C-, 25D-, 25H-, 25I- and 25T2-NBOMe via LC-MS-MS: method validation and analyte stability, J. Anal. Toxicol. 38 (8) (2014) 479–484.
[16] J.L. Poklis, J. Charles, C.E. Wolf, A. Poklis, High-performance liquid chromatography tandem mass spectrometry method for the determination of 2CC-NBOMe and 25I-NBOMe in human serum, Biomed. Chromatogr. 27 (12) (2013) 1794–1800.
[17] B. Duffau, C. Camargo, M. Kogan, E. Fuentes, B.K. Cassels, Analysis of 25 C NBOMe in seized blotters by HPTLC and GC-MS, J. Chromatogr. Sci. 54 (7) (2016) 1153–1158.
[18] B.J. Lum, J.J. Brophy, D.B. Hibbert, Identification of 4-substituted 2-(4-x-2,5-dimethoxyphenyl)-N-[(2-methoxyphenyl)methyl]ethanamine (25X-NBOMe) and analogues by gas chromatography–mass spectrometry analysis of heptafluorobutyric anhydride (HFBA) derivatives, Aust. J. Forens. Sci. 48 (1) (2015) 59–73.
[19] J.L. Poklis, K.G. Devers, E.F. Arbefeville, J.M. Pearson, E. Houston, A. Poklis, Postmortem detection of 25I-NBOMe [2-(4-iodo-2,5-dimethoxyphenyl)-N-[(2-methoxyphenyl)methyl]ethanamine] in fluids and tissues determined by high performance liquid chromatography with tandem mass spectrometry from a traumatic death, Forensic. Sci. Int. 234 (2014) e14–e20.
[20] J.L. Poklis, C.R. Nanco, M.M. Troendle, C.E. Wolf, A. Poklis, Determination of 4-bromo-2,5-dimethoxy-N-[(2-methoxyphenyl)methyl]-benzeneethanamine (25B-NBOMe) in serum and urine by high performance liquid chromatography with tandem mass spectrometry in a case of severe intoxication, Drug Test Anal. 6 (7–8) (2014) 764–769.
[21] A.T. Caspar, A.G. Helfer, J.A. Michely, V. Auwarter, S.D. Brandt, M.R. Meyer, H.H. Maurer, Studies on the metabolism and toxicological detection of the new psychoactive designer drug 2-(4-iodo-2,5-dimethoxyphenyl)-N-[(2-methoxyphenyl) methyl]ethanamine (25I-NBOMe) in human and rat urine using GC-MS, LC-MS(n), and LC-HR-MS/MS, Anal. Bioanal. Chem. 407 (22) (2015) 6697–6719.
[22] A.F. Iezzoni, M.P. Pritts, Applications of principal component analysis to horticultural research, Hort. Sci. 26 (4) (1991).
[23] J.G. Cruz-Castillo, S. Ganeshanandam, B.R. MacKay, G.S. Lawes, C.R.O. Lawoko, D.J. Woolley, Applications of canonical discriminant analysis in horticultural research, Hort. Sci. 29 (10) (1994) 1115–1119.
[24] A.L. Setser, R. Waddell Smith, Comparison of variable selection methods prior to linear discriminant analysis classification of synthetic phenethylamines and tryptamines, Forens. Chem. 11 (2018) 77–86.
[25] D.N. Harris, S. Hokanson, V. Miller, G.P. Jackson, Fragmentation differences in the EI spectra of three synthetic cannabinoid positional isomers: JWH-250, JWH-302, and JWH-201, Int. J. Mass Spectrom. 368 (2014) 23–29.
[26] J. Bonetti, Mass spectral differentiation of positional isomers using multivariate statistics, Forens. Chem. 9 (2018) 50–61.
[27] H.-U. Baier, Shortening analysis time (Fast GC), in: K. Dettmer-Wilde, W. Engewald (Eds.), Practical Gas Chromatography, Springer, New York, NY, 2014, pp. 413–459.
[28] M.S. Klee, L.M. Blumberg, Theoretical and practical aspects of fast gas chromatography and method translation, J. Chromatogr. Sci. 40 (2002) 234–247.
[29] R. Hůšková, E. Matisová, M. Kirchner, Fast GC–ms pesticide multiresidue analysis of apples, Chromatogr. Supp. 68 (2008).
[30] C.C. Chang, G.R. Her, On-line monitoring trihalomethanes in chlorinated water by membrane introduction–fast gas chromatography mass–spectrometry, J. Chromatogr. A 893 (2000) 169–175.
[31] J. Ecker, M. Scherer, G. Schmitz, G. Liebisch, A rapid GC-MS method for quantification of positional and geometric isomers of fatty acid methyl esters, J. Chromatogr. B Analyt. Technol. Biomed Life Sci. 897 (2012) 98–104.
[32] S. Rana, V.P. Uralets, W. Ross, A new method for simultaneous determination of cyclic antidepressants and their metabolites in urine using enzymatic hydrolysis and fast GC-MS, J. Anal. Toxicol. 32 (2008) 355–363.
[33] G. Matz, W. Schroder, A. Harder, A. Schillings, P. Rechenbach, Fast on-site GC/MS analysis of hazardous compound emissions from fires and chemical accidents, Field Anal. Chem. Technol. 1 (4) (1997) 181–194.
[34] A.A. Marais, J.B. Laurens, Rapid GC-MS confirmation of amphetamines in urine by extractive acylation, Forensic Sci Int 183 (1–3) (2009) 78–86.
[35] S. Strano-Rossi, A.M. Bermejo, X. de la Torre, F. Botre, Fast GC-MS method for the simultaneous screening of THC-COOH, cocaine, opiates and analogues including buprenorphine and fentanyl, and their metabolites in urine, Anal. Bioanal. Chem. 399 (4) (2011) 1623–1630.
[36] M.P. Elie, L.E. Elie, M.G. Baron, Keeping pace with NPS releases: fast GC-MS screening of legal high products, Drug. Test. Anal. 5 (5) (2013) 281–290.
[37] K. Kelly, S. Brooks, S. Bell, The effect of mass spectrometry tuning frequency and criteria on ion relative abundances of cathinones and cannabinoids, Forens. Chem. 12 (2019) 58–65.
[38] J.T. Davidson, B.J. Lum, G. Nano, G.P. Jackson, Comparison of measured and recommended acceptance criteria for the analysis of seized drugs using Gas Chromatography-Mass Spectrometry (GC-MS), Forens. Chem. 10 (2018) 15–26.
[39] F.W. McLafferty, D.A. Stauffer, S.Y. Loh, C. Wesdemiotis, Unknown identification using reference mass spectra. Quality evaluation of databases, J. Am. Soc. Mass Spectrom. 10 (1999) 1229–1240.
[40] V.D. Dool, H. Kratz, A generalization of the retention index system including linear temperature programmed gas-liquid partition chromatography, J. Chromatogra. 11 (1963) 463–471.
[41] E. Stauffer, J.A. Dolan, R. Newman, Gas chromatography and gas chromatography–mass spectrometry, Fire Debris Analysis, 1st ed., Elsevier Science & Technology, 2007.
[42] K. Kelly, S. Bell, Evaluation of the reproducibility and repeatability of GCMS retention indices and mass spectra of novel psychoactive substances, Forens. Chem. 7 (2018) 10–18.
[43] Automated Mass Spectral Deconvolution and Identification System (AMDIS), version 2.70; National Institute of Standards and Technology (NIST): Gaithersburg, MD, 2011.
[44] D. Zuba, K. Sekula, Analytical characterization of three hallucinogenic N-(2-methoxy)benzyl derivatives of the 2C-series of phenethylamine drugs, Drug. Test. Anal. 5 (8) (2013) 634–645.
[45] J. Brodbelt, C.-C. Lion, T. Donovan, Selective adduct formation by dimethyl ether chemical ionization in a quadrupole ion trap mass spectrometer and a conventional ion source, Anal. Chem. 63 (13) (1991) 1205–1209.
[46] R.G. Cooks, M. Bertrand, J.H. Beynon, E. Rennekamp, D.W. Setser, Energy partitioning data as an ion structure probe substituted anisoles, J. Am. Chem. Soc. 95 (6) (1973).
[47] F. Meyer, A.G. Harrison, An electron impact study of methyl phenyl ethers, Can. J. Chem. 42 (1964) 2008–2017.
[48] Z. Pelah, H. Budzikiewicz, M. Ohashi, J.M. Wilson, C. Djerassi, Mass spectrometry in structural and stereochemical problems. 34. Aromatic methyl and ethyl ethers, Tetrahedron 19 (12) (1963) 2233–2240.
[49] C. Barnes, J. Occolowitz, The mass spectra of phenyl methyl ethers, Aust. J. Chem. 16 (1963) 219–224.
[50] F.W. McLafferty, M.M. Bursey, Substituent effects in unimolecular ion decompositions. VIII. Rearrangement ions in the mass spectra of substituted phenyl methyl ethers, J. Org. Chem. 33 (1) (1968) 124–127.

[51] T. Awad, J. DeRuiter, C.R. Clark, Gas chromatography-mass spectrometry analysis of regioisomeric ring substituted methoxy methyl phenylacetones, J. Chromatogr. Sci. 45 (2007).
[52] D. Blachut, W. Danikiewicz, M. Olejnik, Z. Czarnocki, Electron ionization mass spectrometry as a tool for the investigation of the ortho effect in fragmentation of some Schiff bases derived from amphetamine analogs, J. Mass Spectrom. 39 (8) (2004) 966–972.